Origin of Enantioselectivity in Palladium-Catalyzed Asymmetric Allylic Alkylation Reactions Using Aminophosphine Ligands

Michael Widhalm,*[,1a] Ulrike Nettekoven,[1a] Hermann Kalchhauser,[1a] Kurt Mereiter,[1b] Maria José Calhorda,*[,1c] and Vítor Félix[1d]

Institut für Organische Chemie, Universität Wien, Währingerstrasse 38, A-1090 Wien, Austria, Institut für Mineralogie, Kristallographie und Strukturchemie, Technische Universität Wien, Getreidemarkt 9, A-1040 Wien, Austria, ITQB, Avenida da República, EAN, Apart. 127, 2781-901 Oeiras, Portugal, Departamento de Química e Bioquímica, Faculdade de Ciências, Universidade de Lisboa, 1749-016 Lisboa, Portugal, and Departamento de Química, Universidade de Aveiro, 3810-193 Aveiro, Portugal

Received June 20, 2001

The asymmetric induction observed in palladium-catalyzed allylic alkylation reactions with typical substrates was investigated using three structurally related chiral PN ligands, which all contain a binaphthyl unit and either a benzyl (**1**) or ferrocenylmethyl (**2**, **3**) fragment bridging phosphorus and nitrogen complexation sites. The intermediate allyl palladium(II) complexes of ligands **1**−**3** have been isolated and spectroscopically characterized. For two of them, **1K** and **3K**, the crystal structure has been determined. A rationalization of the experimental findings on a molecular level is proposed based on the results of DFT (ADF) and molecular mechanics (CERIUS2) calculations. Studies on both the entire molecules and simpler models indicate that the stereochemical outcome is not determined by electronic effects, but mostly by a delicate balance of steric repulsions. In particular, the presence of a benzyl or a ferrocenylmethyl group in the chelate chain has a strong effect on its arrangement, thereby directly influencing asymmetric induction.

Introduction

Recently, the mechanism of the catalytic asymmetric allylic substitution promoted by palladium complexes has been widely discussed; however, some controversy still remains.[2−15] A simplified catalytic cycle for PN ligands, comprising one phosphorus and one nitrogen donor atom and 1,3-symmetrically disubstituted allylic substrates, is outlined in Scheme 1. According to the accepted mechanism, oxidative addition of the racemic substrate leads to the formation of two diastereomeric Pd-(η^3-allyl) complexes with *syn*−*syn* geometry (so-called *exo* and *endo* isomers) that may originate from either of the substrate enantiomers.[2−4]

The palladium complexes may either interconvert via an allyl (pseudo)rotation (Csp^3−Pd) or rearrange to *syn*−*anti* isomers via a η^3-η^1-η^3 mechanism (Csp^2−Csp^3). The catalytic cycle is completed by attack of a soft nucleophile at the more reactive allylic carbon atom. The observed enantioselectivity will depend on the relative concentration of the allylic intermediates under catalytic conditions and on the site selectivity of the nucleophilic attack.

To elucidate the origin of enantioselectivity, several crucial questions have to be addressed, in particular, (1) Which geometric isomers of the allyl complexes are present under catalytic conditions? (2) What is their reactivity toward nucleophilic attack in order to contribute to the product composition? (3) Is the (thermodynamically) more stable allyl complex also the more reactive one? (4) Is the reactivity of the terminal allylic carbons determined by electronic or by steric features?

For PN-donors it has been argued that owing to either electronic reasons (*trans* effect of P) or a combination of electronic and steric interactions the attack should take place predominantly at C3, the carbon atom *trans* to phosphorus.[5,7,16,17] Only in one case has this been

(1) Corresponding authors. E-mail: m.widhalm@univie.ac.at and mjc@itqb.unl.pt. (a) Universität Wien. (b) Technische Universität Wien. (c) ITQB and Universidade de Lisboa. (d) Universidade de Aveiro.

(2) Trost, B. M.; Van Vranken, D. L. *Chem. Rev.* **1996**, *96*, 395.
(3) Auburn, P. R.; Mackenzie, P. B.; Bosnich, B. *J. Am. Chem. Soc.* **1985**, *107*, 2033.
(4) Mackenzie, P. B.; Whelan, J.; Bosnich, B. *J. Am. Chem. Soc.* **1985**, *107*, 2046.
(5) Sprinz, J.; Kiefer, M.; Helmchen, G.; Reggelin, M.; Huttner, G.; Walter, O.; Zsolnai, L. *Tetrahedron Lett.* **1994**, *35*, 1523.
(6) Brown, J. M.; Hulmes, D. I.; Guiry, P. J. *Tetrahedron* **1994**, *50*, 4493.
(7) Togni, A.; Burckhardt, U.; Gramlich, V.; Pregosin, P. S.; Salzmann, R. *J. Am. Chem.* Soc. **1996**, *118*, 1031.
(8) Blöchl, P. E.; Togni, A. *Organometallics* **1996**, *15*, 4125.
(9) Helmchen, G.; Kudis, S.; Sennhenn, P.; Steinhagen, H. *Pure Appl. Chem.* **1997**, *69*, 513.
(10) Pregosin, P. S.; Trabesinger, G. *J. Chem. Soc., Dalton Trans.* **1998**, 727.
(11) Lloyd-Jones, G. C.; Stephen, S. C. *Chem. Eur. J.* **1998**, *4*, 2539.
(12) Helmchen, G. *J. Organomet. Chem.* **1999**, *576*, 203.
(13) Trost, B. M.; Toste, F. D. *J. Am. Chem. Soc.* **1999**, *121*, 4545.
(14) Dierkes, P.; Ramdeehul, S.; Barloy, L.; De Cian, A.; Fischer, J.; Kamer, P. C. J.; Van Leeuwen, P. W. N. M.; Osborn, J. *Angew. Chem., Int. Ed.* **1998**, *37*, 3116.
(15) Ramdeehul, S.; Dierkes, P.; Aguado, R.; Kamer, P. C. J.; Van Leeuwen, P. W. N. M.; Osborn, J. *Angew. Chem., Int. Ed.* **1998**, *37*, 3118.
(16) Allen, J. V.; Coote, S. J.; Dawson, G. J.; Frost, C. G.; Martin, C. J.; Williams, J. M. J. *J. Chem. Soc., Perkin Trans. 1* **1994**, 2065.

10.1021/om0105369 CCC: $22.00
Publication on Web 12/18/2001

Scheme 1. General Mechanism for Pd-Catalyzed Allylic Substitution Reactions with PN-Ligands, Symmetrical Substrates, and Soft Nucleophiles

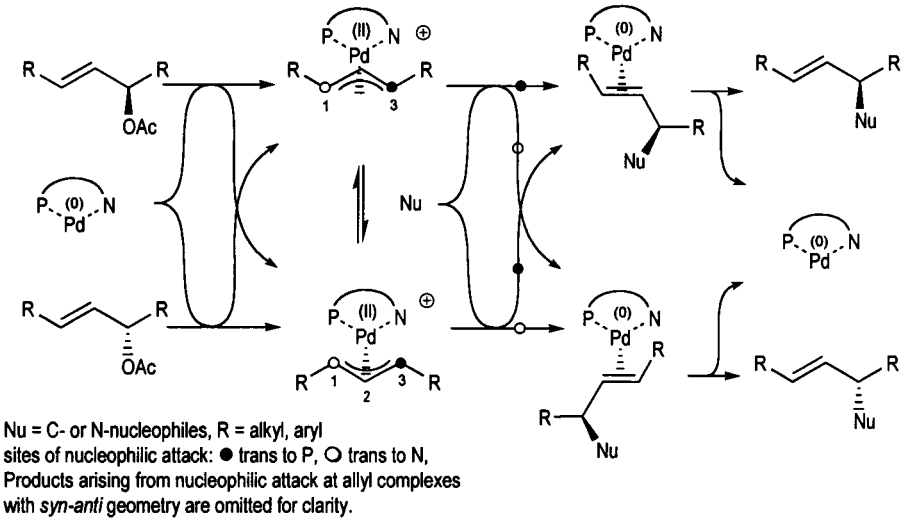

unambiguously evidenced by NMR spectroscopy[18,19] The enantioselectivity would then originate from the different reactivity of diastereomeric allyl complexes and/or their relative amounts. The situation is more complicated if steric and electronic effects favor different allylic carbon atoms. In any case, the characteristics of the rate-determining second step, the nucleophile attack, will generally influence the relative rates of the formation of enantiomeric products.

Much theoretical work has dealt with such aspects;[8,20−27] however, molecular mechanics calculations[28,29] have been used to a great extent, but address only steric factors, while quantum chemical methods have been applied only to relatively small models. The large size and absence of symmetry of the catalytic systems, however, require large models, which are difficult to handle.

The present work reports results of asymmetric allylic substitution reactions with palladium complexes of azepine-type PN-ligands **1**,[30] **2**,[31] and **3**[31] (Scheme 2). All of them contain a 2,2′-bridged binaphthyl entity as

Scheme 2

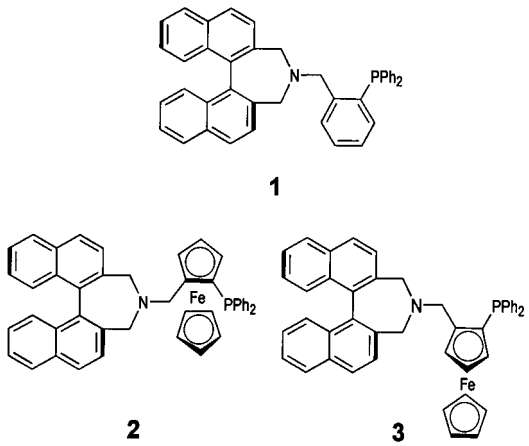

1 **2** **3**

the asymmetry-inducing element, but differ with respect to a benzyl (**1**) or ferrocenyl (**2**, **3**) moiety linking P and N complexation sites. Despite the apparently similar structures of their palladium complexes as determined by crystal structure analyses, their reactivity and asymmetric induction proved to be surprisingly different. A rationalization of their significantly dissimilar behavior in catalysis and elucidation of the origin of their asymmetric induction will be given, based on the combined results of NMR investigations and DFT[32] (ADF program[33]) and molecular mechanics calculations using the universal force field[34] within the CERIUS2 graphical interface.[35]

Results

Catalytic Experiments. Results of asymmetric allylic alkylations (Scheme 3) using dimethyl malonate as the nucleophile and palladium complexes prepared in situ from the corresponding ligands **1**, **2**, or **3** and

(17) Dawson, G. J.; Williams, J. M. J.; Coote, S. J. *Tetrahedron: Asymmetry* **1995**, *6*, 2535.
(18) Steinhagen, H.; Reggelin, M.; Helmchen, G. *Angew. Chem., Int. Ed. Engl.* **1997**, *36*, 2108.
(19) Junker, J.; Reif, B.; Steinhagen, H.; Junker, B.; Felli, I. C.; Reggelin, M.; Griesinger, C. *Chem. Eur. J.* **2000**, *6*, 3281.
(20) Dedieu, A. *Chem. Rev.* **2000**, *100*, 543.
(21) Branchadell, V.; Moreno-Mañas, M.; Pajuelo, F.; Pleixats, R. *Organometallics* **1999**, *18*, 4934.
(22) Magistrato, A.; Merlin, M.; Pregosin, P. S.; Rothlisberger, U.; Albinati, A. *Organometallics* **2000**, *19*, 3591.
(23) Delbecq, F.; Lapouge, C. *Organometallics* **2000**, *19*, 2716.
(24) Svensson, M.; Bremberg, U.; Hallman, K.; Csöregh, I.; Moberg, C. *Organometallics* **1999**, *18*, 4900.
(25) Canal, J. M.; Goméz, M.; Jiménez, F.; Rocamora, M.; Muller, G.; Duñach, E.; Franco, D.; Jiménez, A.; Cano, F. H. *Organometallics* **2000**, *19*, 966.
(26) Evans, D. A.; Campos, K. C.; Tedrow, J. S.; Michael, F. E.; Gagné, M. R. *J. Am. Chem. Soc.* **2000**, *122*, 7905.
(27) Liu, S.; Müller, J. F. K.; Neuburger, M.; Schaffner, S.; Zehnder, M. *Helv. Chim. Acta* **2000**, *83*, 1256.
(28) Oslob, J. D.; Åkermark, B.; Helquist, P.; Norrby, P.-O. *Organometallics* **1997**, *16*, 3015.
(29) Hagelin, H.; Svensson, M.; Åkermark, B.; Norrby, P.-O. *Organometallics* **1999**, *18*, 4574.
(30) (a) Wimmer, P.; Widhalm, M. *Tetrahedron: Asymmetry* **1995**, *6*, 657. (b) Wimmer, P.; Widhalm, M. *Monatsh. Chem.* **1996**, *127*, 669.
(31) Widhalm, M.; Nettekoven, U.; Mereiter, K. *Tetrahedron: Asymmetry* **1999**, *10*, 4369.
(32) Parr, R. G.; Yang, W. *Density Functional Theory of Atoms and Molecules*; Oxford University Press: New York, 1989.
(33) *Amsterdam Density Functional (ADF) program*, release 2.3; Vrije Universiteit: Amsterdam, The Netherlands, 1995.
(34) Rappé, A. K.; Casewit, C. J.; Colwell, K. S.; Goddard, W. A., III; Skiff, W. M. *J. Am. Chem. Soc.* **1992**, *114*, 10024.
(35) *CERIUS2*, version 4.0; Molecular Simulations Inc: San Diego, 1999.

Scheme 3

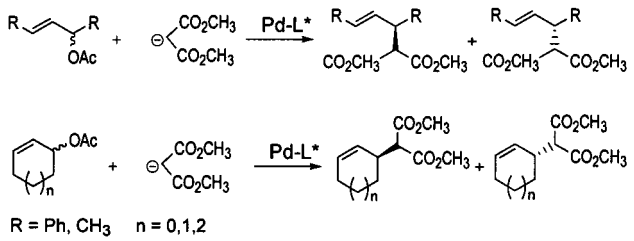

Table 1. Enantioselectivities in Allylic Alkylation Reactions

substrate	ligand configuration		
	(S_a)-**1**	(S_a,R_m)-**2**	(S_a,S_m)-**3**
(*E*)-1,3-diphenylprop-2-en-1-yl acetate	**97 (*S*)**	54 (*S*)	44 (*S*)
(*E*)-pent-3-en-2-yl acetae	5 (*R*)	33 (*R*)	**37 (*R*)**
cyclopent-2-en-1-yl acetate	15 (*R*)	37 (*S*)	**71 (*R*)**
cyclohex-2-en-1-yl acetate	28 (*R*)	**49 (*S*)**	36 (*R*)
cyclohept-2-en-1-yl acetate	63 (*R*)	**66 (*S*)**	56 (*R*)

$[Pd(\eta^3\text{-}C_3H_5)Cl]_2$ in CH_2Cl_2 are listed in Table 1. For the synthesis of ligands and a detailed experimental procedure for catalytic experiments see refs 30, 31, and 36.

In the alkylation of (*E*)-1,3-diphenylprop-3-en-1-yl acetate all ligands with (S_a) configuration afforded products with (*S*) configuration, albeit with a different degree of asymmetric induction. Particularly for **2** and **3** with opposite metallocene configuration this was unexpected and clearly demonstrates that the ferrocene moiety occupies a position too remote from the complexation site of the substrate to exert a marked influence on the asymmetric induction. Interestingly, employing pent-3-en-2-yl acetate, the reversed product configuration[37] was found, accompanied by improved enantioselectivity induced by ferrocene ligands **2** and **3**. In contrast, for cyclic substrates which form η^3-allyl complexes with *anti*−*anti* geometry, the configuration of the products is predominantly controlled by the ferrocene rather than by the binaphthyl configuration.[38] Thus, ligands with (R_m) configuration afford cycloalkenyl malonate with (*S*) configuration.

Synthesis of Complexes. The cationic palladium allyl complexes [(1,3-diphenyl-η^3-allyl)(**1**)Pd]BF_4, **1K**, [(1,3-diphenyl-η^3-allyl)(**2**)Pd]BF_4, **2K**, and [(1,3-diphenyl-η^3-allyl)(**3**)Pd]BF_4, **3K**, were prepared from the corresponding ligands, palladium-1,3-diphenyl-η^3-allyl acetate dimer, and silver tetrafluoroborate[39] and isolated as crystalline orange solids. For two of them, **1K** and **3K**, the solid-state structure could be determined (see below).

NMR Investigations. A detailed investigation of **1K**, **2K**, and **3K** at low temperatures using one- and two-dimensional NMR methods was performed,[40] showing a C_1-symmetrical binaphthyl moiety in agreement with a chelate structure for all compounds. When dissolving the crude precipitate of the tetrafluoroborate complex **1K** in $CDCl_3$, a mixture of two main isomers A and B in a ratio of 62:38 was observed in ^{1}H NMR. Small amounts of other species (<10%) were also detected but could not be analyzed due to signal broadening. Upon dissolving a crystal from the batch used in crystal structure analysis at low temperature (−20 °C, quick filtration over Celite), the NMR spectrum showed the predominance of A (∼90%) between −50 and −10 °C. With this sample, the kinetics of equilibration were followed at 0 °C but were found to be in poor agreement with a first-order process. The equilibrium, which was reached after 1.5 h, was A:B = 74:26, differing significantly from the value mentioned above.[41] For the main product A the assignment of most of the ^{1}H and ^{13}C resonances was possible. NOEs confirmed the *syn*−*syn* geometry of the substrate and permitted the identification of the Ph-allyl proximate to the binaphthyl moiety. At −60 °C the rotation of this phenyl ring is frozen.

For **2K** only one distinct species (approximately 80%) was detected in ^{1}H NMR, showing several coalescence phenomena between −50 and 20 °C. Moreover, an undefined number of other species, presumably allyl complexes, gave rise to broad resonances. Only a limited number of signals of the main compound could be assigned. Again *syn*−*syn* geometry, evidenced by a NOE between CH_A and CH_C of the allyl fragment, was found, and the rotation of one of the allyl-Ph rings was frozen at −50 °C.

The ^{1}H NMR spectrum of **3K** in $CDCl_3$ was not conclusive; several species were present, but broad and poorly resolved multiplets at room temperature prevented any assignment. From integration of the Cp signals at −60 °C the presence of four species in a ratio of 38:23:19:19 was found, but only signals due to the main product became sharp and enabled partial assignment. As evidenced from NOESY spectra, the two main species exhibit *syn*−*syn* geometry. It is interesting to note that the simultaneous appearance of NOEs between the terminal methine allyl groups (CH_A−CH_C), one terminal and one central group (CH_A−CH_B), and between a terminal group and the Cp ring cannot originate from a single species. These findings rather indicate the presence of three structures in equilibrium (see Supporting Information).

Crystallographic Studies. The crystal structures of the cationic complexes **1K**·$(CH_3)_2CO$ (enantiopure) and **3K**·CH_3OH (racemic) obtained from (*S*)-**1** and (S_a*,S_m*)-**3** were determined by X-ray diffraction (Figure 1, Figure 2).

Both complexes exhibit the typical distorted square planar arrangement of PN chelates of Pd with bite angles of 93.1° (**1K**) and 95.4° (**3K**) and similar bond

(36) Widhalm, M.; Wimmer, P.; Klintschar, G. *J. Organomet. Chem.* **1996**, *523*, 167.

(37) Concerning the absolute configuration of the product see: Vyskocil, S.; Smrcina, M.; Hanuš, V.; Polášek, M.; Kocovský, P. *J. Org. Chem.* **1998**, *63*, 7738.

(38) Similar concepts have been reported using a cymantrene or chromium tricarbonyl arene bridge to link P and N coordination sites: (a) Kudis, S.; Helmchen, G. *Angew. Chem.* **1998**, *110*, 3210. (b) Schleich, S.; Helmchen, G. *Eur. J. Org. Chem.* **1999**, 2515. (c) Han, J. W.; Jang, H.-Y.; Chung, Y. K. *Tetrahedron: Asymmetry* **1999**, *10*, 2853.

(39) Hayashi, T.; Yamamoto, A.; Ito, Y.; Nishioka, E.; Miura, H.; Yanagi, K. *J. Am. Chem. Soc.* **1989**, *111*, 6301.

(40) Pregosin, P. S.; Salzmann, R. *Coord. Chem. Rev.* **1996**, *155*, 35.

(41) Assuming a first-order kinetics an approximate rate constant $k_1 \approx 2.0 \times 10^{-4}$ s^{-1} is calculated with an equilibrium constant $K = 0.35$. Being surprisingly slow, this equilibration process is assumed to be accelerated under catalytic conditions. Solvent and anion dependence of the interconversion of palladium allyl complexes have been reported, and indeed, recording the spectrum of **1K** in CD_2Cl_2 at room temperature revealed an A:B ratio of 90:10 (see ref 5 and Gogoll, A.; Örnebro, J.; Grennberg, H.; Bäckvall, J.-E. *J. Am. Chem. Soc.* **1994**, *116*, 3631). The study of a possible enhancement of complex isomerization in the presence of acetate was attempted; however, in situ preparation from palladium-1,3-diphenyl-η^3-allyl acetate dimer and **1** failed, due to complex decomposition above −10 °C.

lengths for Pd−N (2.23 and 2.20 Å) and Pd−P (2.29 and 2.30 Å). Some evidence for steric strain was detected in both complexes but proved to be more pronounced in **3K**, where the angle C51−C4−N opened to 120.9°, a value considerably larger than that of 115.2° in **1K**. The desymmetrization of the complexes measured by the difference in the terminal allyl carbon−palladium distances was similar for **1K** and **3K** (0.14 Å), indicating a weaker palladium−carbon bond *trans* to phosphorus. Envelope-like conformations were found in both cases, but different orientation of the bridging aryl resulted in an entirely different geometry of the chelate ring. The allyl ligand exhibits an *exo* configuration in **1K** and shows the *endo* configuration in **3K**. Also steric interactions between ligand and phenyl substituents of the allyl cause a rotation of the allylic unit. The coplanarity of aromatic portions in the PN and in the allylic ligand, suggested by crystal structure analyses and NMR investigations,[42] forces different degrees of distortions onto the η^3-allyl moiety.

DFT Calculations. DFT calculations[32] (ADF program[33]) were performed on two of the allyl cations with *syn*−*syn* geometry[43] (Scheme 4), **1**-exosynsyn and the **1**-endosynsyn analogue (see Experimental Section for details). The energy difference between these two isomeric compounds was found to be 19 kJ mol^{-1}, the *exo* isomer being the more stable and thus the predominating species under the reaction conditions ($K_{endo/exo} = 3.85 \times 10^{-4}$). The optimized structure of the **1**-exosynsyn complex was in good agreement with the crystal structure of **1K**. Some relevant distances and angles are given in Table 2 and compared with the experimental values.

The complexity and size of these structures, containing over 100 atoms, prevented a general application of ab initio methods to all species of interest within reasonable calculation time. To explore the possible existence of other isomers in a more convenient way, the chiral carbon backbone was simplified as depicted in Scheme 5. The study of such model structures was necessary to check their reliability in mimicking the core geometry of real complexes and to separate conformational changes due to steric interaction of peripheral aromatic groups from stereoelectronic effects operating closer to the central atom.

Geometry optimization of these models was carried out for the *exo*−*syn*−*syn* and *endo*−*syn*−*syn* arrangements (referred to as **M1**-exosynsyn and **M1**-endosynsyn), as well as for the previously unconsidered *exo*−*syn*−*anti* and *endo*−*syn*−*anti* isomers (**M1**-exosynanti and **M1**-endosynanti). The other possible isomers were eliminated based on a first screening using molecular mechanics calculations, owing to their much higher energy (see below). The relative energies of these species and selected structural parameters are also listed in Table 2.

Scheme 4. Structures of Isomeric Pd Allyl Complexes of 1 and 3[43]

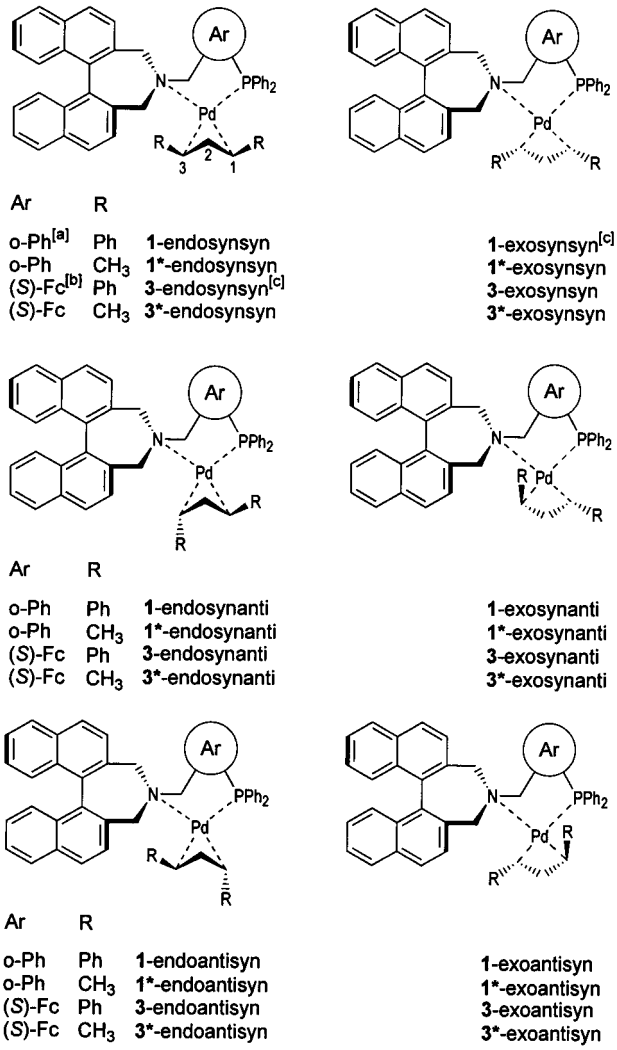

[a] o-Ph = 1,2-phenylene [b] (*S*)-Fc = 1,2-$C_5H_3FeC_5H_5$ [c] crystal structure

The *exo*−*syn*−*syn* isomer was again found to be the most stable one among the model structures considered. Interestingly, the geometric deviations relative to the optimized complete structure (and also the experimental one) seem negligible (**M1**-exosynsyn versus **1**-exosynsyn), as depicted in Figure 3a, which displays an overlay of these two structures. The same good agreement was observed for the complete structure and the model of the *endo*−*syn*−*syn* isomer (Figure 3b). The models reproduce the features of the complete structures in a reliable way, namely, the coordination environment of the metal and the chelate ring (the core of the complex), some slightly larger deviations being observed near the periphery. These deviations can be traced back to interactions between aromatic rings, which were partly removed in the models. Calculations were also performed for several isomers of ferrocene complexes of **3K** (Scheme 4). Taking into account the previous results and the fact that the number of atoms is even larger, only models with the same approximations as above were used in the calculations on this series of compounds, namely, **M3**-endosynsyn and **M3**-exosynsyn (Scheme 5).

M3-exosynsyn is more stable by 9 kJ mol^{-1} than **M3**-endosynsyn, although the latter exhibits the same

(42) Hunter, C. A.; Sanders, J. K. M. *J. Am. Chem. Soc.* **1990**, *112*, 5525.

(43) Nomenclature: Structures are denoted *exo* or *endo* if substituents of the allyl part are located remote or proximate to the binaphthyl moiety. According to ref 7, the sequence of numbering the ally part starts with C1 *cis* to P, C2 for the central carbon, and C3 *trans* to P. Consequently the first geometric descriptor, *syn* or *anti*, refers to the configuration of a non-H substituent at C1 relative to H-C2, the second one for a substituent at C3 relative to H-C2. Olefin complexes are denoted with the extension "-o1" or "-o3" for attack of the nucleophile at C1 or C3, respectively.

Table 2. Calculated (DFT) Distances (Å), Angles (deg), and Relative Energies (kJ mol^{-1})[a] of 1K, Pd-1,3-Diphenylallyl Complexes 1 and M1, and Corresponding Olefin Complexes M4

	1K solid state	**1**-exo synsyn	**M1**-exo synsyn	**M1**-exo synanti	**1**-endo synsyn	**M1**-endo synsyn	**M1**-endo synanti	**M4**-exo synsyn-o1	**M4**-exo synsyn-o3
ΔE/kJ mol^{-1}		0	0	26.7	19.2	9.1	28.4	0	21.2
N−Pd	2.227	2.297	2.297	2.280	2.310	2.305	2.271	2.387	2.478
P−Pd	2.292	2.349	2.340	2.345	2.343	2.319	2.332	2.319	2.322
C3−Pd	2.307	2.378	2.336	2.339	2.448	2.421	2.326	2.217	3.319
C2−Pd	2.185	2.292	2.230	2.188	2.276	2.264	2.197	2.159	2.249
C1−Pd	2.171	2.250	2.227	2.241	2.249	2.223	2.275	3.144	2.152
C1−C2	1.415	1.420	1.421	1.424	1.422	1.426	1.425	1.517	1.415
C2−C3	1.391	1.405	1.410	1.419	1.400	1.401	1.410	1.421	1.527
C1−C11	1.487	1.474	1.473	1.472	1.469	1.479	1.471	1.523	1.484
C3−C21	1.455	1.468	1.468	1.479	1.464	1.465	1.495	1.479	1.518
N−Pd−P	93.1	92.3	91.3	90.7	91.9	90.6	91.7	88.4	88.3
N−Pd−C3	103.7	104.3	105.3	107.7	106.6	108.3	103.6	113.5	111.0
P−Pd−C1	97.2	98.9	98.0	96.0	96.9	96.7	99.2	102.2	109.2
C1−C2−C3	121.6	122.4	121.1	122.0	121.1	122.4	123.2	121.1	122.3

[a] For atom labeling see Figure 1.

Scheme 5. Model Structures of Pd Allyl Complexes 1 and 3

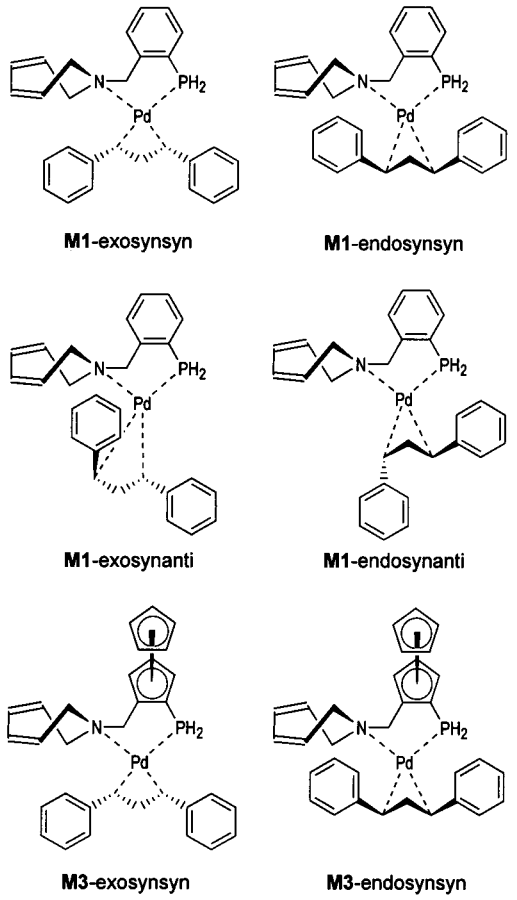

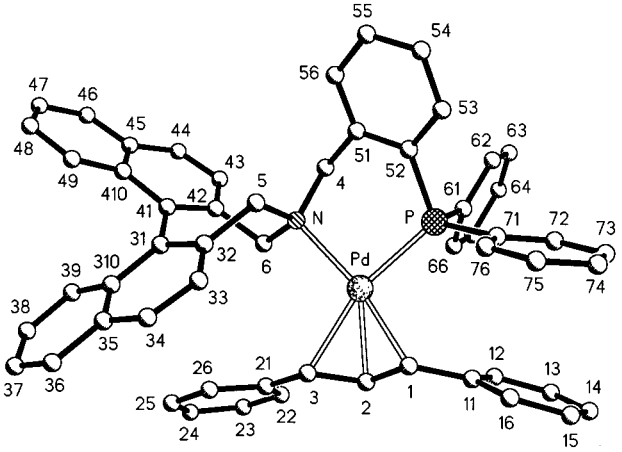

Figure 1. Selected geometric data of **1K** in crystalline **1K**·$(CH_3)_2CO$ (Å, deg): N−Pd = 2.227, P−Pd = 2.292, C3−Pd = 2.307, C2−Pd = 2.185, C1−Pd = 2.171, C1−C2 = 1.415, C2−C3 = 1.391, C1−C11 = 1.487, C3−C21 = 1.455, N−Pd−P = 93.09, N−Pd−C3 = 103.73, P−Pd−C1 = 97.18, C1−C2−C3 = 121.57, binaphthyl angle = 55.88, C51−C4−N = 115.24, C32−C5−N = 115.03, C42−C6−N = 113.92, deviation from plane N−Pd−P = 0.284 (C1), 0.022 (C3), deviation from plane C1−C2−C3 = 0.082 (C11), 0.052 (C21), plane angle N−Pd−P/C1−C2−C3 = 112.1, plane angle C11−C1−C2/C11···C16 = 37.6, plane angle C2−C3−C21/C21.C26 = 16.9, plane angle N−Pd−P and "bridging aryl" = 142.3.

arrangement as found in the crystal structure. Upon overlaying **M3**-endosynsyn and the crystal structure of **3K**, the reasons became obvious. Whereas the cores of the two molecules overlap perfectly (the calculated rms for the three allylic carbons atoms, Pd, N, and P, is 0.070 Å), the phenyl rings of the allyl fragment are rotated in a different mode, owing to the absence of steric repulsion between them and the binaphthyl rings (the calculated rms value increases to 0.275 Å upon addition of the other core atoms).

As observed in other structures, the presence of the phenyl rings attached to P and in the naphthyl fragment forces the allylic phenyl rings also to adapt in order to minimize steric repulsions, while the remaining part of the molecule barely changes.

M3-exosynsyn also overlaps extremely well with the core atoms of **3K** (*endo*−*syn*−*syn* configuration), namely, the twisted seven-membered ring. Thus the (unsubstituted) dihydroazepine makes a suitable model for the much larger binaphthyl group for the purpose of performing quantum chemistry calculations. Indeed, the closest H···H contact distances at ∼3 Å are kept in the model. It should be stressed that the calculated energy difference between the two isomers is only 9 kJ mol^{-1}, a value of the same order of magnitude as van der Waals interactions. Taking into account all the substituents, such small energy difference can easily be overcome (see molecular mechanics calculations below).

The next aspect to address deals with the effect on the core geometry of the complexes upon replacing the bridging phenylene group (**1**) by a ferrocene unit (**3**).

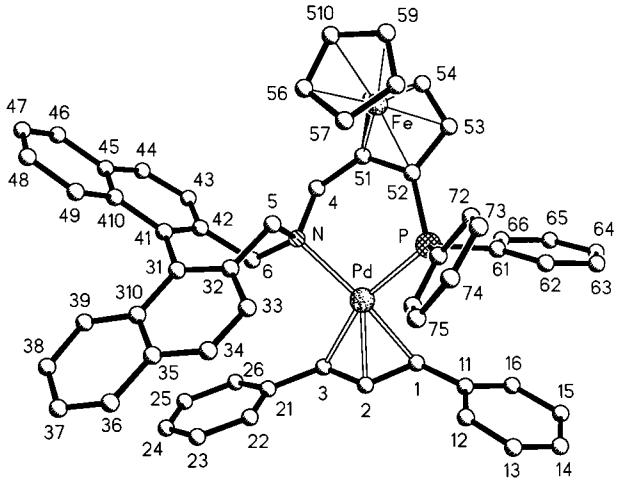

Figure 2. Selected geometric data of **3K** in crystalline racemic **3K**·CH_3OH (Å, deg): N−Pd = 2.202, P−Pd = 2.301, C3−Pd = 2.328, C2−Pd = 2.188, C1−Pd = 2.185, C1−C2 = 1.399, C2−C3 = 1.310, C1−C11 = 1.443, C3−C21 = 1.496, N−Pd−P = 95.43, N−Pd−C3 = 102.22, P−Pd−C1 = 96.88, C1−C2−C3 = 126.88, binaphthyl angle = 58.38, C51−C4−N = 120.87, C32−C5−N = 112.47, C42−C6−N = 114.61, deviation from plane N−Pd−P = 0.412 (C1), 0.195 (C3), deviation from plane C1−C2−C3 = 0.135 (C11), 0.079 (C21), plane angle N−Pd−P/C1−C2−C3 = 119.2, plane angle C11−C1−C2/C11···C16 = 36.9, plane angle C2−C3−C21/C21···C26 = 23.7, plane angle N−Pd−P and "bridging aryl" = 212.3.

Superimposing structures of related pairs of complexes, namely, **M1**-exosynsyn versus **M3**-exosynsyn, and **M1**-endosynsyn versus **M3**-endosynsyn, suggests that the coordination mode of the allylic ligand does not affect the core geometry. Furthermore, modification of the aromatic moiety, namely, the inclusion of a phenylene or a ferrocenyl unit, does not alter the core geometry, in what concerns distances and angles, but dramatically changes the conformation of the chelate ring. Envelope conformations were found in all cases, but with different "up/down" orientations of the aromatic rings. This resulted in stronger steric interaction for **M1**-type species, concomitant with an apparent twist of the azepine part, while **M3** species adopted a sterically less demanding geometry. These geometric differences arise from different bond angles in Ph and Cp. The orientation of the second Cp ring is not particularly important, thus the metallocene chirality will not influence the conformation. This is in agreement with very similar enantioselectivities observed in the allylic alkylation reaction using ligand **2** or **3** (Table 1).

To have an insight into the preferred position for nucleophilic attack, the nature of the charge distribution and the LUMO composition was determined, as they are relevant for a charge-controlled or an orbitally controlled reaction, respectively. For all compounds studied, the charge distribution indicates a very small difference between the two terminal allyl carbon atoms. The LUMO of **1**-exosynsyn is mainly localized on several d orbitals of Pd (∼20%) and on the two terminal allylic carbons C1 (15%) and C3 (14%), the remaining being scattered among many other atoms in very small amounts. The composition is very similar for other isomers (models and complete structures). The difference of localization of the LUMO among the two terminal carbon atoms of the allyl is negligible and does not point toward an obvious position of nucleophilic attack, in case the reaction was orbitally controlled.

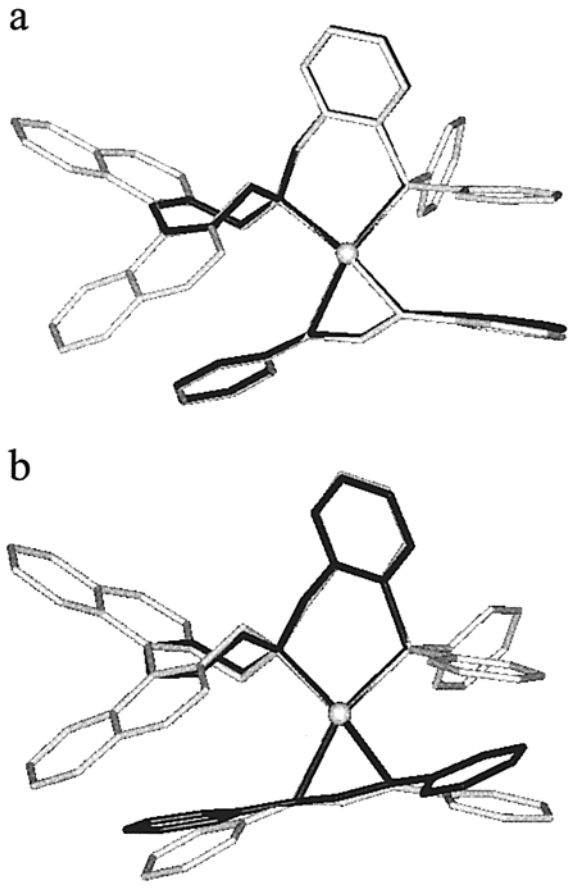

Figure 3. Superimposed complete structures and model structures from DFT calculations of (a) **1**-exosynsyn (gray) with **M1**-exosynsyn (black) and (b) **1**-endosynsyn (gray) with **M1**-endosynsyn (black).

DFT calculations also addressed the problem of relative stabilities of olefin Pd(0) complexes originating from the nucleophilic attack at one of the terminal carbon atoms of the coordinated η^3-allyl (Scheme 1). Hydride was chosen as the nucleophile. Our approach was to identify the most likely allylic precursor and the favored position of attack, from which implications for the reaction mechanism could be derived.

Calculations were performed using the models **M4** and **M5**, formally representing products derived from **M1** and **M3**, respectively. Both sites of nucleophilic attack, *trans* to N (**M4**-exosynsyn-o1) or *trans* to P (**M4**-exosynsyn-o3), were considered (Scheme 6). Selected parameters of calculated structures are listed in Table 2. It is interesting to note that the products arising from attack at C_{allyl} *trans* to N are by far more stable.

The enthalpy change, ΔH, of the reaction *allylic complex + hydride → olefin complex* was calculated for several systems and is given in Table 3. These values may be overestimated owing to the use of hydride, instead of another nucleophile. Solvent effects may also play an important role, as the charges of the complexes vary during the reaction, but all systems should be similarly affected.

All reactions were found to be exothermic and, more strongly, when the attack took place *trans* to N. Indeed,

Scheme 6. Model Structures of Pd(0) Olefin Complexes of 1 and 3

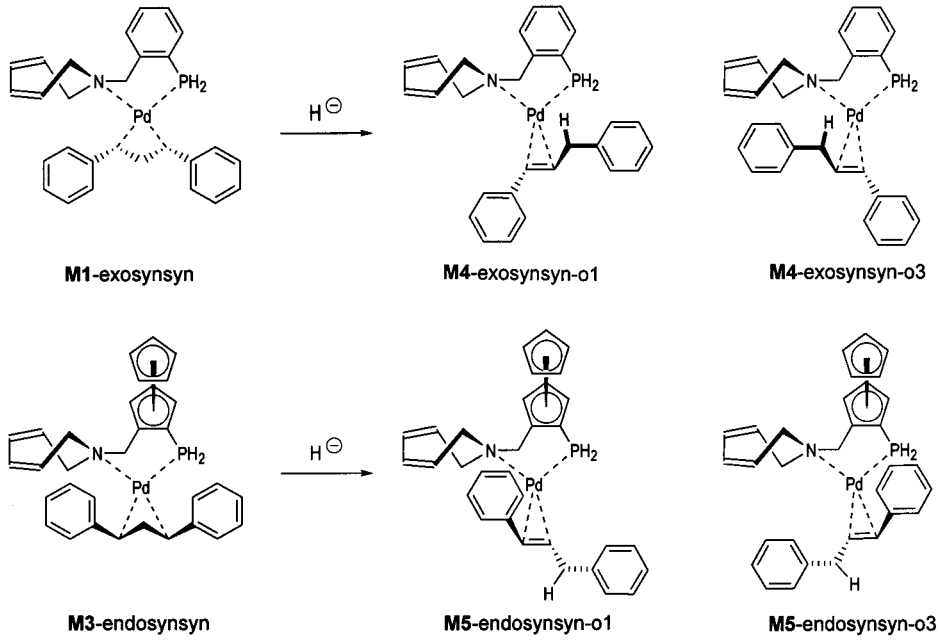

Table 3. Enthalpy Changes (kJ mol^{-1}) in the Reaction Allylic Complex + Hydride → Olefin Complex

		ΔH/kJ mol^{-1}	
allyl complex	olefin complex	attack *trans* to N	attack *trans* to P
1-exosynsyn	**4**-exosynsyn-o3		−706.7
1-endosynsyn	**4**-endosynsyn-o3		−689.6
M1-exosynsyn	**M4**-exosynsyn-o3		−717.2
	M4-exosynsyn-o1	−738.1	
M3-endosynsyn	**M5**-endosynsyn-o3		−721.4
	M5-endosynsyn-o1	−740.2	

the values given in Table 3 reflect the relative energies of the final olefin complexes, obtained from the same precursor.

Molecular Mechanics Calculations. Since results of DFT calculations showed that the energy differences between isomeric allyl complexes were only a few kJ mol^{-1}, the order of stability of different isomers might be reversed when taking into account the full bulk of the substituents. In all cases studied the core geometry remained basically unchanged, indicating that electronic effects did not vary much. This opened the possibility of performing molecular mechanics (MM) calculations[28,29] for detailed investigations on the complete structures of likely catalytic intermediates, provided that reasonable constraints were introduced to fix the coordination geometry at the palladium atom.

(a) Allyl- and Olefin-Pd Complexes Derived from 1 and 1,3-Diphenylallyl. Calculations were performed on four isomers: **1**-exosynsyn, **1**-exosynanti, **1**-endosynsyn, and **1**-endosynanti (Scheme 4). Several other geometrical isomers have been excluded from a detailed investigation because of their extraordinarily high energy in preliminary calculations. Relative energies are listed in Table 4. Comparing geometries of **1**-exosynsyn and **1**-endosynsyn, obtained with either DFT or MM methods, a satisfactory agreement was observed in general with the better fit obtained for the *exo* isomer

Table 4. Calculated (MM) Relative Energies (kJ mol^{-1}) and Estimated Equilibrium Concentrations of Pd-Allyl Complexes 1, 3, 1*, and 3*, and Corresponding Olefin Complexes Derived Therefrom by Reaction with Dimethyl Malonate

allyl complex	ΔE	equilibrium concentration	olefin complex	ΔE
1-exosynsyn	0	>99%	**4**-exosynsyn-o1	0.0
			4-exosynsyn-o3	8.3
1-exosynanti	27.0	0%		
1-endosynsyn	18.2	<1%		
1-endosynanti	15.1	<1%		
3-exosynsyn	29.0	0%		
3-exosynanti	29.5	0%		
3-endosynsyn	4.4	15%	**5**-endosynsyn-o1	0.0
			5-endosynsyn-o3	104.5
3-endosynanti	13.1	<1%		
3-endoantisyn	0.0	85%	**5**-endoantisyn-o1	
1*-exosynsyn	5.8	9%	**4***-exosynsyn-o1	0.0
			4*-exosynsyn-o3	9.6
1*-exosynanti	7.6	4%		
1*-endosynsyn	0.0	86%	**4***-endosynsyn-o1	2.2
			4*-endosynsyn-o3	0.0
1*-endosynanti	13.5	<1%		
1*-endoantisyn	12.5	<1%		
3*-exosynsyn	11.0	1%		
3*-exosynanti	7.5	4%		
3*-endosynsyn	4.1	15%	**5***-endosynsyn-o1	7.3
			5*-endosynsyn-o3	0.0
3*-endosynanti	0.0	76%	**5***-endosynanti-o3	
3*-endoantisyn	7.3	4%		

with rms = 0.331 Å (for all non-H atoms; i.e., 0.0056 Å per atom).

Again, MM calculations point toward **1**-exosynsyn as the highly predominating species if in equilibrium with corresponding *endo* and/or *anti* isomers. The surprisingly near perfect agreement of energy differences calculated by DFT and MM methods is noteworthy.

Next, relative energies and structures of Pd(0) olefin complexes formed from **1**-exosynsyn and dimethyl malonate were investigated. Depending on the site of attack, either *trans* to N or *trans* to P, complexes **4**-exosynsyn-o1 and **4**-exosynsyn-o3 were considered (Scheme

Scheme 7. Diphenylallyl Complexes of (*S*)-1 and Reaction with Soft Nucleophiles Forming Pd(0) Olefin Intermediates

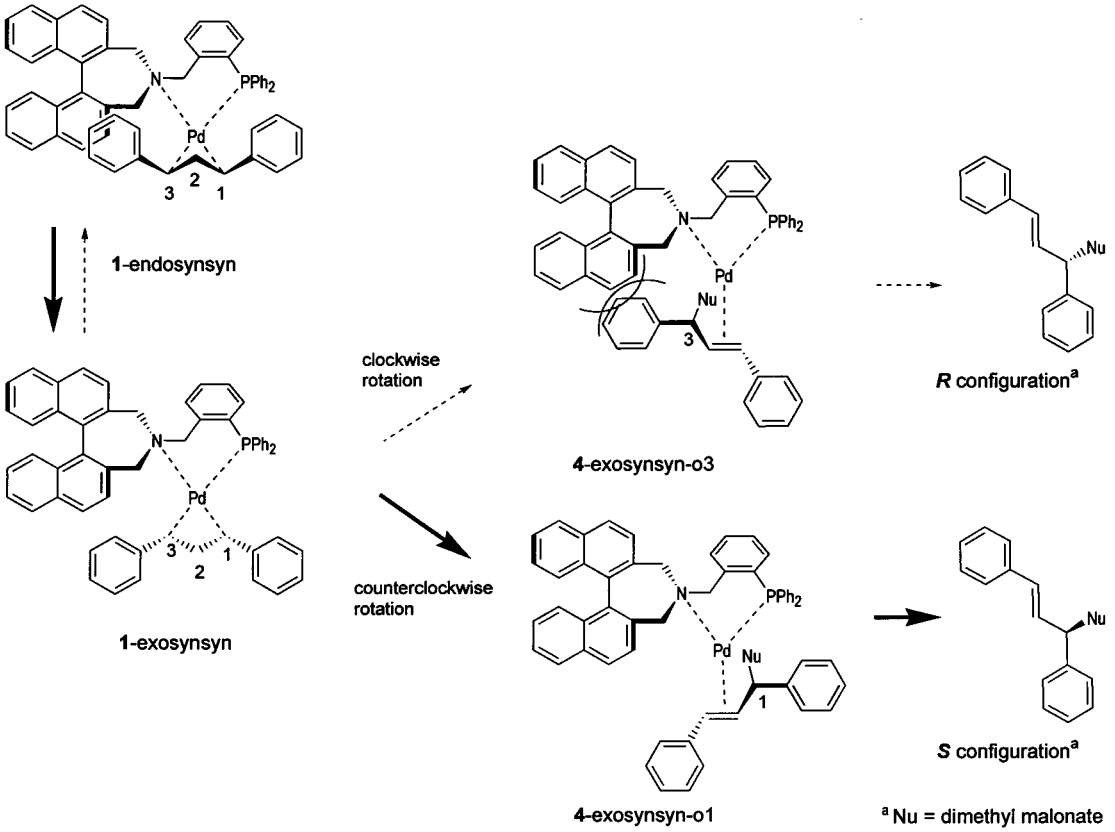

7). The results parallel those from DFT calculations of corresponding model structures, but energy differences are less pronounced due to the use of the bulkier dimethyl malonate instead of hydride (Table 4).

(b) Allyl and Olefin Pd Complexes Derived from 3 and 1,3-Diphenylallyl. Similar calculations were performed for five allyl complexes of ligand **3** (Scheme 4, Table 4), revealing that the geometry of the crystal structure is fairly reproduced by MM calculations of **3**-endosynsyn with rms = 0.664 Å. This is an acceptable agreement regarding the quality of data from the X-ray structure analysis. As suggested from the solid structure, this isomer represents one of the low-energy species and is found to be ~25 kJ mol^{-1} more stable than **3**-exosynsyn. Surprisingly, its stability is even surpassed by that of **3**-endoantisyn, although the difference is small (~4 kJ mol^{-1}). In the case of the ligand **3**, three olefin complexes that are formed from either **3**-endosynsyn or **3**-endoantisyn had to be investigated. For the latter, only attack at C1 (*trans* to N) gives the observed product bearing a double bond with (*E*) configuration. Next, we considered the relative stabilities of analogous Pd complexes bearing a 1,3-dimethylallyl ligand, the proposed intermediates in the allylation reaction with (*E*)-pent-3-en-2-yl acetate.

(c) Allyl and Olefin Pd Complexes Derived from 1 and 1,3-Dimethylallyl. The energy differences between 1,3-methyl-substituted Pd-allyl complexes are low, and species with *anti* configuration are disfavored (Scheme 4, notation "*" indicates the change of substituents methyl for phenyl; Table 4). The complex with *endo*−*syn*−*syn* geometry predominates, and two other species, with *exo*−*syn*−*syn* (9%) and *exo*−*syn*−*anti* arrangement (4%), are present to a small extent.

(d) Allyl and Olefin Pd Complexes Derived from 3 and 1,3-Dimethylallyl. In this case, **3***-endosynanti predominates (76%), and **3***-endosynsyn should be present in lower concentration (15%) (Scheme 4, Table 4). The situation is complicated by the finding that the most stable allyl complex (reagent) forms a high-energy olefin complex (**5***-endosynanti-o3), which should result in an increased activation barrier. This might slow the rate for this reaction path to such an extent that a minor isomer like **3***-exosynsyn could become the main carrier of the reaction.

Discussion

For complex **1K**, the expected predominance of a single species was evidenced from NMR experiments. Its *exo*−*syn*−*syn* configuration was confirmed by a NOE between H1 and H3 and matches the crystal structure. A similar NOE between the terminal allyl protons of a minor compound indicates an *endo*−*syn*−*syn* geometry. The ratio of the two complexes, measured in CD_2Cl_2, is 9:1, which is in acceptable agreement with experimental results and DFT and MM calculations.

For complexes with ferrocene ligands, **2K** and **3K**, only one isomer with *syn*−*syn* geometry predominates in each case. Moreover, with **3K**, two additional NOEs were found which might originate from the presence of two other species in fast equilibrium, namely, the other *syn*−*syn* and the *endo*−*anti*−*syn* species.[44] We assigned the *endo* configuration to the main allyl complex (**3**-endosynsyn, the same as in the crystal structure), from

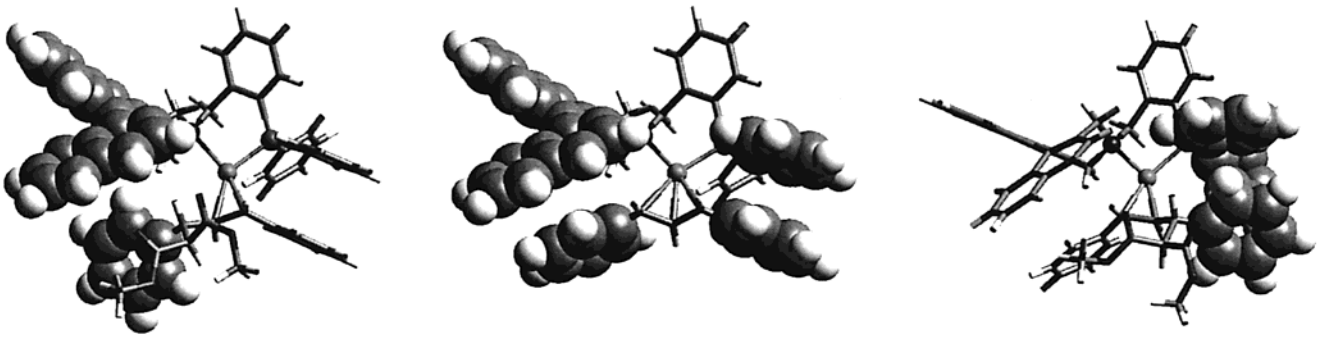

Figure 4. Structure of the Pd-allyl complex of **1** (**1**-exosynsyn, center) and the olefin complexes **4**-exosynsyn-o1 (right) and **4**-exosynsyn-o3 (left), emphasizing the phenyl rings of the ligands and the strongest repulsions between them.

which two new species may arise, either through a C−C rotation or a C−Pd rotation in intermediate η^1-allyl complexes to give **3**-endoantisyn and **3**-exosynsyn. This hypothesis explains the observed NOEs and agrees well with calculation results.

The general mechanism outlined in Scheme 1 implies a change from an η^3-allyl complex to an η^2-olefin complex, where only two carbon atoms remain bound to the metal. Therefore, besides other subtler changes, a shift of the C_3 chain to the left or to the right will take place, giving rise to different steric repulsions between the olefin and the binaphthyl or the phosphine phenyl groups. It should be taken into account that no strong preference for one of the allylic carbon atoms, based on either charge or orbital control of the reaction, was found (DFT calculations). Thus, geometric rearrangements induced by steric effects will play a determining role in the reaction outcome.

First it has to be decided which allyl complexes have sufficiently low energy to be present in reasonable equilibrium concentration under experimental conditions. For practical reasons we included only species that are present in more than 1% amounts. For the system with ligand **1** and a 1,3-diphenylallyl fragment both experimental evidence (crystal structure analysis and NMR studies) and calculation results (DFT and MM) suggest **1**-exosynsyn to be the most likely precursor of the nucleophilic attack. The observed enantioselectivity with this system implies a high preference in reactivity of C1 over C3.

The observed site selectivity can be rationalized by comparing the geometry of the starting material (**1**-exosynsyn) with two possible products (**4**-exosynsyn-o1 and **4**-exosynsyn-o3). The system requires a more dramatic rearrangement to go from **1**-exosynsyn to **4**-exosynsyn-o3 than to **4**-exosynsyn-o1. This is reflected by very different rms values of 1.043 and 0.645 Å, respectively. It appears that the energy differences between the olefin complexes are caused by different degrees of steric interaction between aromatic rings. This is exemplified in Figure 4, where the steric repulsions between phenyl rings are shown in the allyl complex (**1**-exosynsyn, center) and in the two products of nucleophilic attack by malonate (**4**-exosynsyn-o3, left, and **4**-exosynsyn-o1, right). It can be seen that the repulsions are minimized in the allyl complex (rings approximately parallel). Attack at C1 leads to a shift of the ligand to the right (only two carbons remain coordinated to the Pd), increasing the steric repulsions between phenyl rings (olefin and phosphine). On the other hand, attack at C3 results in a shift to the left, and stronger repulsions develop between the phenyl rings of the olefin and the binaphthyl. That the latter are stronger can be seen from the orientation of the double bond, which is significantly rotated away from the P−Pd−N plane. The d^{10} Pd center would prefer a planar arrangement.[45] As the nucleophile addition step is highly exothermic and the starting state is the same for both processes, a stabilizing effect on the product will, to some extent, stabilize the preceding transition state.

Summarizing, two major effects contribute to the site selectivity. The first concerns steric interactions modified by the geometric rearrangement of the allyl to the olefin complex, reflected by their deviations from ideal geometries. The second derives from the desymmetrization in the allyl complex which may anticipate the forthcoming rearrangement. As the reagent transforms into the product along the reaction coordinate, one of the competing pathways is favored, because the geometry of one possible product (**4**-exosynsyn-o1) is much closer to that of the starting complex. Thus, a lower activation energy can be expected (principle of least motion).[7,46]

Similar considerations were applied to the analogous system with ligand **3**, exhibiting less enantiocontrol. It can be estimated from MM calculations that two species, **3**-endosynsyn and **3**-endoantisyn, are predominant and coexist in a ratio of 15:85. Again, steric interactions seem to determine the relative stabilities of the allyl complexes. The effect of the ferrocenyl group replacing the phenylene ring is a dramatic one regarding the conformation of the chelate, whereas direct steric interaction with the unsubstituted Cp ring is low.

On moving to systems with *meso*-like η^3-pentenyl ligands, differing from the previous ones by replacing the phenyl groups on the allyl ligand by methyls, energy differences between isomers are smaller. For both ligands, **1** and **3**, one allyl complex predominates, but in addition several other isomers with comparable energy are present too (1−15%). For **1***-endosynsyn it turned out that, irrespectively of the pronounced desymmetrization, the asymmetric induction is negligible.

(44) A scheme providing a mechanistic rationalization of this finding can be found in the Supporting Information.

(45) Albright, T. A.; Burdett, J. K.; Whangbo, M.-H. *Orbital Interactions in Chemistry*; Wiley: New York, 1985.

(46) The principle of least motion, see: Hine, J. *Adv. Phys. Org. Chem.* **1977**, *15*, 1.

Scheme 8. Allylic Substitution with Cyclic Substrates

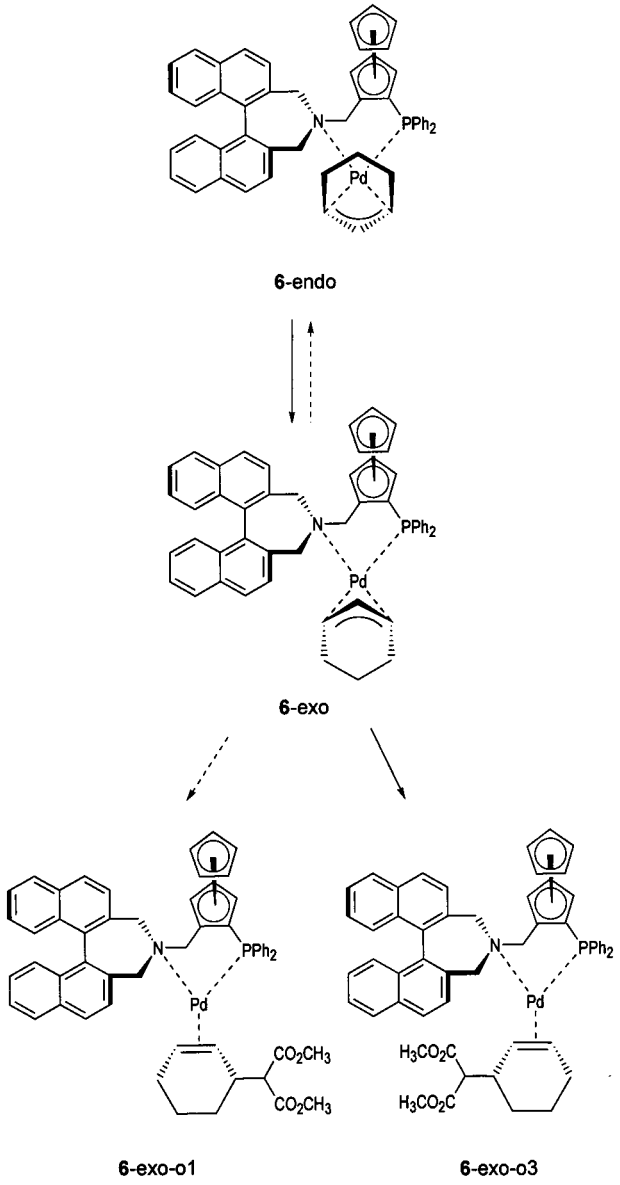

This is probably a consequence of very similar energies of olefin complexes derived from the starting allyl complexes. Since the torsional barrier of an η^3-allyl complex near its ideal geometry (within ~20°) is low,[45] deformations do not always reflect severe steric interactions. For ligand **1**, the predominance of **1***-endosynsyn with pronounced desymmetrization is not sufficient to induce satisfactory enantiodiscrimination. The derived olefin complexes differ only slightly in energy, herewith explaining the negligible enantioselectivity (Table 1). In case of ligand **3**, the situation is similarly complicated by the presence of several allyl complexes exhibiting different site selectivities. If desymmetrization effects and relative stabilities of products point toward different reaction pathways and, moreover, more than one allyl complex is present, it is difficult to quantify their relative influence on the system.

For cyclic substrates the geometric situation is completely different. On the basis of the previous knowledge and from inspection of a wire model for ligand **3** it can be inferred that only one of the two possible allyl complexes should be stable, namely, the one in which the main part of the substrate is located "*anti*" to the unsubstituted Cp ring.[12,14] This isomer (**6**-exo) is depicted in Scheme 8 for a cyclohexenyl ligand. The transformation of the allyl complex to the olefin complex represents formally a clockwise or counterclockwise rotation. Since in both cases cycloolefin complexes of very similar steric interaction are formed, the electronic effects might control the stereochemical outcome. A nucleophilic attack *trans* to P giving **6**-exo-o3 is in agreement with the experimental findings.

Conclusions

The combined use of DFT and MM calculations provided a detailed insight into the geometric properties of large chiral allyl- and olefin-Pd complexes, which are often important intermediates in asymmetric synthesis. The origin of enantiocontrol in the palladium-catalyzed allylic substitution reaction depends on catalyst and substrate structure. Typically, steric interactions dominate, favoring the exclusive or predominant formation of one allylic intermediate.[47] In the majority of cases the site selectivity of the second step is determined by the choice of a reaction path providing minimum steric interference[48] during the geometric rearrangement from a η^3-allyl palladium complex to a η^2-olefin palladium complex. Relative preferences can be predicted from desymmetrization of the allyl moiety and, more important, from relative stabilities of the product complexes. Electronic effects will play an important role only in the absence of steric control, as exemplified with cyclic substrates. Expectedly, the moderate enantioselectivities observed with the linear aliphatic substrate (*E*)-pent-3-en-2-yl acetate can be explained by the coexistence of several allylic intermediates, giving rise to olefinic products with similar energy content.

The distinctly dissimilar performances of ligands **1** and **3** are a consequence of different chelate conformation. A direct steric interaction of the Cp ring with the coordinated substrate is less likely except for cyclic substrates where the metallocene configuration determines the configuration of the product.

The combination of DFT and force field calculations is a useful tool to rationalize the different performances of structurally related catalytic systems, provided the (general) mechanism is known and manifold catalytic cycles are operating at different rate only from different steric interactions. These findings open the way for fine-tuning the structures of new chiral auxiliaries for specific synthetic applications, thereby avoiding extensive screening experiments.

Experimental Section

Chiral ligands **1**,[30] **2**, and **3**[31] were prepared as described elsewhere. The numbering of NMR spectra followed the labeling scheme used for the crystal structures (see Figures 1 and 2).

Allylic substitution experiments were performed under standard conditions as described in the literature.[36] Enantio-

(47) For the role of $\pi-\pi$ stacking interactions in palladium complexes see: Magistrato, A.; Pregosin, P. S.; Albinati, A.; Rothlisberger, U. *Organometallics* **2001**, *20*, 4178.

(48) Saitoh, A.; Achiwa, K.; Tanaka, K.; Morimoto, T. *J. Org. Chem.* **2000**, *65*, 4227.

meric excesses of products were determined by chiral GC and HPLC.[36,49]

Synthesis of Palladium Allyl Complexes (Typical Procedure). 1,3-Diphenylallyl palladium acetate dimer[39] (18 mg, 0.05 mmol) and $AgBF_4$ (10 mg, 0.05 mmol) were stirred in 1 mL of acetone. After 0.5 h, the supernatant pale yellow solution was filtered through a short pad of Celite to a stirred solution of **3** (34 mg, 0.05 mmol) in 1 mL of CH_2Cl_2. Washings of the precipitated silver acetate (acetone, 1 mL) were added, whereupon the dark solution became turbid and finally a yellow precipitate formed. The precipitate was separated, washed with ether, and dried in vacuo, yield 43 mg (81%) of **3K**.

NMR Experiments. NMR spectra were obtained from approximately 5−10 mg samples in $CDCl_3$ or CD_2Cl_2 on Bruker DRX 400 WB (^{1}H, 400 MHz; ^{13}C, 100 MHz; ^{31}P, 161.9 MHz) and DRX 600 (^{1}H, 600 MHz; ^{13}C, 150 MHz; ^{31}P, 242.9 MHz) spectrometers in 5 mm tubes and are referenced to internal TMS using the solvent resonances as secondary standards (^{1}H, ^{13}C; 7.24/77.0 ppm for $CDCl_3$, 5.33/53.7 ppm for CD_2Cl_2) or to 85% external H_3PO_4 (^{31}P).

Crystal Structure Determination. X-ray data were collected on a Siemens/Bruker SMART three-circle diffractometer with a CCD area detector and graphite-monochromatized Mo Kα radiation ($\lambda = 0.71073$ Å). Corrections for absorption were semiempirically from equivalent reflections. Structure solution was by direct methods, refinement by full-matrix least-squares on F^2. **1K**·$(CH_3)_2CO$ (enantiopure): $C_{59}H_{51}BF_4NOPPd$, M_r = 1014.19, monoclinic, space group $P2_1$ (no. 4), a = 9.334(3) Å, b = 10.290(4) Å, c = 26.165(7) Å, β = 95.37(1)°, V = 2502.0(14) Å^3, Z = 2, D_c = 1.346 Mg m^{-3}, T = 295(2) K, μ = 0.46 mm^{-1}, independent reflections 10 737, parameters 654, final R1 = 0.033 (all data), wR2 = 0.077 (all data). **3K**·CH_3OH (racemic): $C_{61}H_{53}BF_4FeNOPPd$, M_r = 1096.07, monoclinic, space group $P2_1/c$ (no. 14), a = 13.274(6) Å, b = 21.590(10) Å, c = 18.501(8) Å, β = 107.03(2)°, V = 5070(4) Å^3, Z = 4, D_c = 1.436 Mg m^{-3}, T = 299(2) K, μ = 0.73 mm^{-1}, independent reflections 6517, parameters 641, final R1 = 0.117 (all data), wR2 = 0.158 (all data). Further details are given in the Supporting Information.

DFT Calculations. Density functional calculations[32] were carried out with the Amsterdam Density Functional (ADF) program[33] developed by Baerends and co-workers (release 2.3).[50] Vosko, Wilk, and Nusair's local exchange correlation potential was used,[51] with Becke's nonlocal exchange[52] and Perdew's correlation corrections.[53] The geometry optimization procedure was based on the method developed by Versluis and Ziegler,[54] using the nonlocal correction terms in the calculation of the gradients. The coordinates of the X-ray determined structure of complex **1K** were taken for the first calculation (**1**-exosynsyn), and the CERIUS2 program was used to build the other isomer and the models (see Schemes 5 and 6). All the structures were fully optimized.

In all the calculations, a triple-ζ Slater-type orbital (STO) basis set was used for Pd 5s, 4p, 5p, 4d; for C, N 2s and 2p; and for P 3s and 3p. A double-ζ STO basis set was used for H 1s. A frozen core approximation was used to treat the core electrons of C, N (1s), P (1s, 2s, 2p), and Pd ([1−3]s, [1−3]p, 3d).

MM Calculations. Molecular mechanics (MM) calculations were carried out using the CERIUS2 software[35] on a silicon graphics IRIX 6.3 workstation. Default Universal Force Field was used.[34] Charges were taken into account and are included via the charge equilibration method using the Qeq-charge 1.1 parameter set available from the CERIUS2 version used. The starting geometries of all isomeric structures were built either from the corresponding cores optimized by DFT calculations, keeping their geometries and then adding the aromatic parts, or from X-ray structure analysis, or from complete structures optimized by DFT calculation.

All structures were minimized employing the steepest descendent gradient followed by the Newton Rhapson gradient until convergence was achieved. High convergence criteria with default parameters were used. For all isomers the geometric arrangement around the palladium center was fixed during the minimization process, namely, the atomic coordinates of the metal center, the nitrogen, the phosphorus, and the two carbon and four hydrogen atoms of the olefinic system, or the three carbon and three hydrogen atoms of the allylic system, respectively. In addition, for isomeric ferrocenyl derivatives of type **3** and **5**, the ferrocenyl moiety was treated as a rigid body in calculations.

Acknowledgment. This work was supported by the Fonds zur Förderung der wissenschaftlichen Forschung (FWF), project No P-11990CHE, and by the PRAXIS XXI under project PRAXIS/PCNA/C/QUI/103/96. M.J.C. and M.W. thank the ÖAD for a travel grant. M.J.C. thanks the TMR Transition Metal Clusters in Catalysis and Organic Synthesis. V.F. thanks the British Council and FCT for funding.

Supporting Information Available: Experimental details of NMR measurements, structure comparison (in tabulated form (4 Tables) and as overlay drawings (5 Figures)), mechanistic implications of observed NOEs (1 Scheme), and complete crystallographic data (10 Tables, 4 Figures). This material is available free of charge via the Internet at http://pubs.acs.org.

OM0105369

(49) Xiao, L.; Weissensteiner, W.; Mereiter, K.; Widhalm, M. Manuscript in preparation.
(50) (a) Baerends, E. J.; Ellis, D.; Ros, P. *Chem. Phys.* **1973**, *2*, 41. (b) Baerends, E. J.; Ros, P. *Int. J. Quantum Chem.* **1978**, *S12*, 169. (c) Boerrigter, P. M.; te Velde, G.; Baerends, E. J. *Int. J. Quantum Chem.* **1988**, *33*, 87. (d) te Velde, G.; Baerends, E. J. *J. Comput. Phys.* **1992**, *99*, 84.
(51) Vosko, S. H.; Wilk, L.; Nusair, M. *Can. J. Phys.* **1980**, *58*, 1200.
(52) Becke, A. D. *J. Chem. Phys.* **1987**, *88*, 1053.
(53) (a) Perdew, J. P. *Phys. Rev.* **1986**, *B33*, 8822. (b) Perdew, J. P. *Phys. Rev.* **1986**, *B34*, 7406.
(54) (a) Versluis, L.; Ziegler, T. *J. Chem. Phys.* **1988**, *88*, 322. (b) Fan, L.; Ziegler, T. *J. Chem. Phys.* **1991**, *95*, 7401.